N95-28432

APPLICATION OF ADVANCED MATERIAL SYSTEMS TO COMPOSITE FRAME ELEMENTS

Steven Llorente, Pierre Minguet, Russell Fay
Helicopters Division, Boeing Defense & Space Group
Philadelphia, Pennsylvania
and
Steven Medwin
Composites Division
E.I. Du Pont De Nemours & Company (Inc.)
Wilmington, Delaware

SUMMARY

A three phase program has been conducted to investigate DuPont's Long Discontinuous Fiber (LDF™*) composites. Additional tests were conducted to compare LDF™ composites against toughened thermosets and a baseline thermoset system. Results have shown that the LDF™ AS4/PEKK offers improved interlaminar (flange bending) strength with little reduction in mechanical properties due to the discontinuous nature of the fibers. In the third phase, a series of AS4/PEKK LDF™ C-section curved frames (representing a typical rotorcraft light frame) were designed, manufactured and tested. Specimen reconsolidation after stretch-forming and frame thickness were found to be key factors in this light frame's performance. A finite element model was constructed to correlate frame test results with expected strain levels determined from material property tests. Adequately reconsolidated frames performed well and failed at strain levels at or above baseline thermoset material test strains. Finally a cost study was conducted which has shown that the use of LDF™ for this frame would result in a significant cost savings, for moderate to large lot sizes compared with the hand lay-up of a thermoset frame.

INTRODUCTION

In weight critical applications graphite composite materials provide a highly desirable combination of structural properties since the orientation of the fibers can be selected to suit the application. In general, the hand lay-up of thermoset parts which are contoured is a difficult and time consuming process. Thermoplastic LDF™ materials offer the ability to be thermoformed while maintaining a high percentage of the continuous fiber material properties since fibers are of such a length (approximately 2 inches) that they retain properties similar to continuous fiber composites. The combination of long discontinuous fibers and a thermoplastic matrix produces a material which can be consolidated in stock shapes and then stretch-formed to a final shape. The economics are attractive since the stock shape can be produced efficiently and the final part can be contoured automatically with minimal labor. Most importantly, the fiber angles can be controlled so that they adapt to the part geometry. The general stretch forming concept is shown schematically in Figure 1.

In the first phase of a three phase evaluation, laminate coupon tests were used to evaluate material stiffness and strength properties of the new material system. Emphasis was placed on evaluating the effect of the discontinuous fibers and the effect of stretching on mechanical properties. In the second phase, two types of tests were performed to

* LDF is a trademark of the DuPont Company.

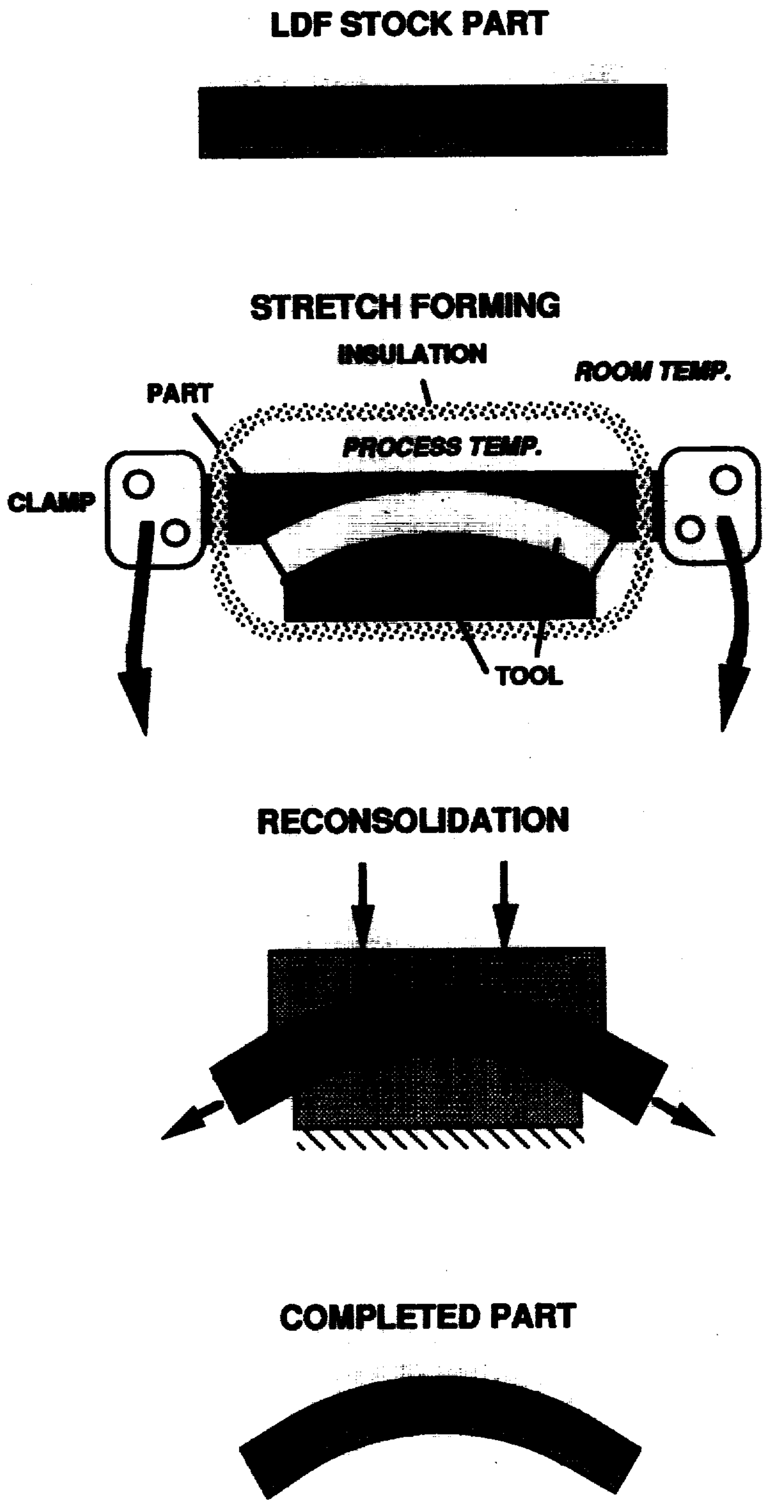

Figure 1 LDF™ Stretch-Forming Concept Definition

evaluate two critical frame failure modes: flange bending and section crippling. In addition to the LDF™ AS4/PEKK, a baseline thermoset, AS4/3501-6, and a toughened thermoset with a high strain-to-failure fiber, T800/3900, were tested for comparison purposes. In the third phase, a series of C-section curved frames manufactured with the LDF™ AS4/PEKK were manufactured and tested in combined tension and bending. To evaluate the results of this frame test, a finite element model was constructed for each frame geometry. Finally a cost study was conducted comparing the LDF™ stretch forming process to hand lay-up. This report presents the results of this investigation and details the manufacturing, testing, and supporting analysis.

PHASE 1 MATERIAL PROPERTIES

In Phase 1, the material stiffness and strength properties of LDF™ composite (AS4/PEKK) were determined through a series of (room temperature-ambient environment) coupon tests and compared with the properties of an AS4/PEKK composite made with continuous fibers. Different layups were tested in tension and compression. Several stretched (20% elongation) LDF™ coupons were also tested to evaluate the effect of stretching on mechanical properties.

The Phase 1 test matrix is shown in Figure 2. A total of 68 specimens were tested in a laboratory environment. Hot/Wet specimens were not tested due to budget restrictions. Tension tests of unidirectional $[0]_8$ and $[90]_8$ laminates were performed to evaluate fiber and matrix dominated properties and laminates of $[\pm45]_{2s}$ and $[\pm45/0/90]_{2s}$ layups were tested to evaluate shear and quasi-isotropic behavior. In all cases except for the $[90]_8$ laminates, both LDF™ and continuous AS4/PEKK laminates were compared. It was not believed that fiber discontinuity would significantly affect 90° behavior. $[0]_8$ and $[\pm45/0/90]_{2s}$ LDF™ specimens stretched by 20% in length were also evaluated.

Compression tests were conducted to determine both the modulus and ultimate strength of unidirectional $[0]_8$ laminates. As with the tension tests, both LDF™ and continuous AS4/PEKK laminates were compared. Finally, the quasi-isotropic $[\pm45/0/90]_{2s}$ layup was evaluated in compression tests to examine the behavior of a typical laminate in the continuous, LDF™ stretched and LDF™ unstretched configuration.

RESULTS

Tension Tests

Results for tension strength and extensional stiffness are shown in Figure 3. A reduction of 5% was observed between continuous and discontinuous fibers specimens which is considered insignificant. The LDF™ stretched specimens showed higher strength, probably due to the slight tapering of these specimens after stretching. Both the LDF™ and LDF™-stretched specimens also experienced a slight reduction in modulus (7%,5%, respectively) due to the discontinuous fibers. The 90° LDF™ specimens failed at an average stress level of 9.5 ksi. For comparison, previous results for similar tests of IM6/3501-6 tape material resulted in an average failure stress of 6.4 ksi.

Layup	Test Type	Specimen Geometry	Number of Specimens: LDF™ Unstretched, RT Dry	LDF™ Unstretched, 180° Wet	LDF™ Stretched, RT Dry	LDF™ Stretched, 180° Wet	Continuous Fiber, RT Dry	Continuous Fiber, 180° Wet
$[0]_8$	Tension ASTM D3039	0.5" x 9.5"	5	5	5	5	3	3
	Compression Strength ASTM D695	0.5" X 3.18"	5	5	5	5	3	3
	Compression Modulus ASTM D695	0.5" x 3.18"	3	3	3	3	3	3
$[90]_{20}$	Tension ASTM D3039	1.0" x 9.5"	5	5	-	-	-	-
$[\pm45]_{2S}$	Tension	1.0" x 9.5"	5	5	-	-	5	5
$[\pm45/0/90]_S$	Tension	0.5" x 9.5"	3	3	3	3	3	3
	Compression	0.5" x 9.5"	3	3	3	3	3	3

Figure 2 Test Matrix for Phase 1 - Material Evaluation

LAYUP	AS4/PEKK Material Type	Strength (KSI)	Coeff. of Variation (%)	Modulus (MSI)	Coeff. of Variation (%)
$[0]_8$	CONT. FIBER	255	6	17.7	3.1
	LDF™	242	6	16.4	6.1
	STRETCHED LDF™	274	5	16.8	21.7
$[90]_8$	LDF™	9.5	19	1.52	1.0
$[\pm45]_{2S}$	CONT. FIBER	16.8	4.5	0.85	4.9
	LDF™	21.0	4.1	0.87	7.8
$[\pm45/0/90]_S$	CONT. FIBER	88	3.7	6.3	9.6
	LDF™	86	3.8	6.4	14.5
	STRETCHED LDF™	54	5.9	5.1	10.9

Figure 3 Average Tension Test Results

The ±45 tension tests showed no reduction in strength or modulus due to the discontinuous fiber. Stress based on actual thickness increased 25%. Finally, in the quasi-isotropic layup the presence of the discontinuous fibers did not significantly reduce strength (2%), while it slightly increased the initial modulus (2%). The stretched specimens were tapered significantly lengthwise; thicknesses ranged from .035"to .042".

Compression Tests

Results for compression strength and extensional stiffness are shown in Figure 4. The LDF™ 0° strength is reduced by 15% while the modulus increased slightly (5%). A degradation of 42% in strength and 4% in stiffness was observed for stretched LDF™ specimens. These values were obtained using nominal thickness. Once again, in the stretched specimens, significant tapering occurred. Finally, in the quasi-isotropic layup the presence of the discontinuous fibers reduced strength by 19% and stretched specimens failed at an average of 38 ksi, a reduction of 65%.

LAYUP	AS4/PEKK Material Type	Strength (KSI)	Coeff. of Variation (%)	Modulus (MSI)	Coeff. of Variation (%)
$[0]_8$	CONT. FIBER	257	3	19.6	9
	LDF™	218	9	20.6	13
	STRETCHED LDF™	149	13	18.9	2
$[+/-45/0/90]_S$	CONT. FIBER	110	5	6.3	10
	LDF™	89	6	7.7	15
	STRETCHED LDF™	38	39	5.1	11

Figure 4 Average Compression Test Results

PHASE 1 DISCUSSION

The Phase 1 stiffness and strength results were useful for determining the effect of the discontinuous fibers of the LDF™ material on basic mechanical properties. These values are in line with DuPont test results reported in the literature[1]. However, the stretched LDF™ specimens suffered from a number of structural problems resulting from the unidirectional draw operation. First, the specimens were severely tapered lengthwise. Second, it is not believed that the consolidation was fully completed after drawing. This was easiest to see from the failed quasi-isotropic compression specimens . The continuous and LDF™ laminates both failed in compressive fracture. The drawn LDF™ specimen failure was due to delamination, a clear indication of poor post-stretch consolidation. These results have indicated that the process used to make flat stretched sheets from which the test specimens were made needs improvement and that this second consolidation is critical to LDF™ part performance.

PHASE 2 STRUCTURAL PROPERTIES

Phase 2 Test Matrix

In Phase 2, structural tests were performed to determine the suitability of LDF™ for curved frames. A series of compression tests on C-channel specimens to examine the buckling and crippling behavior, and a series of flange bending tests to examine the interlaminar strength properties were conducted. For comparison, tests were also performed on specimens made with graphite/epoxy (AS4/3501-6) and a high-strain-to-failure fiber with toughened thermoset (T800/F3900), both in fabric form. The test matrix for the Phase 2 task is shown in Figure 5. For each material type, six channel specimens were tested in compression, three of them undamaged and three damaged with a 1/2 inch impactor at an energy level of five foot-pounds. Three flange bending tests were also conducted for each material type. For comparison, five specimens of each Phase 2 laminate were also tested in compression to determine their in-plane ultimate strength.

	TEST TYPE			
	Channel Crippling 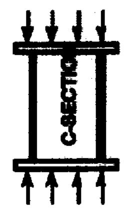		Flange Bending 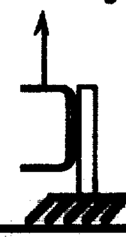	Coupon Compression Ultimate 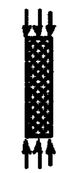
Material System	Undamaged	Damaged	Undamaged	Undamaged
AS4/PEKK LDF™ Tape $[(\pm45)_2/0/90/\pm45/0/90]_S$ 20 plies (.108")	3	3	3	5
AS4/3501-6 Fabric $[45_2/0_2/45_2/0]_S$ 14 plies (.105")	3	3	3	5
T800/F3900 Fabric $[45_2/0/45/0]_S$ 10 plies (.110")	3	3	3	5

Figure 5 Phase 2 Test Matrix

Manufacturing and Testing

<u>Crippling Tests</u>

A tape layup of $[(+45/-45)_2/0/90/+45/-45/0/90]_S$ was chosen for the LDF™ specimens to closely match the orientation of the fabric materials used for comparison. Matched metal tools were utilized. Crippling specimens were potted on each end with a room temperature curing epoxy contained in a 1/2 inch high aluminum ring (Figure 6). The channel crippling specimens were instrumented and then tested in compression after proper specimen alignment. Load was applied at a constant stroke rate until failure. Some crippling specimens were impacted by placing the potted specimen in a fixture which rigidly supported one of the flanges. The impact location is shown in Figure 6. Damage caused by the impact event was measured using ultrasonic NDI (Non Destructive Inspection) methods.

Flange Bending Tests

Flange bending specimens were obtained by cutting c-channel sections into 2.0 inch wide slices and bonding the web to a thick aluminum backing plate. The specimens were loaded through a bolt causing interlaminar tension stresses in the corner. The test was continued until multiple fractures in the radius region occurred, resulting in a significant loss of load.

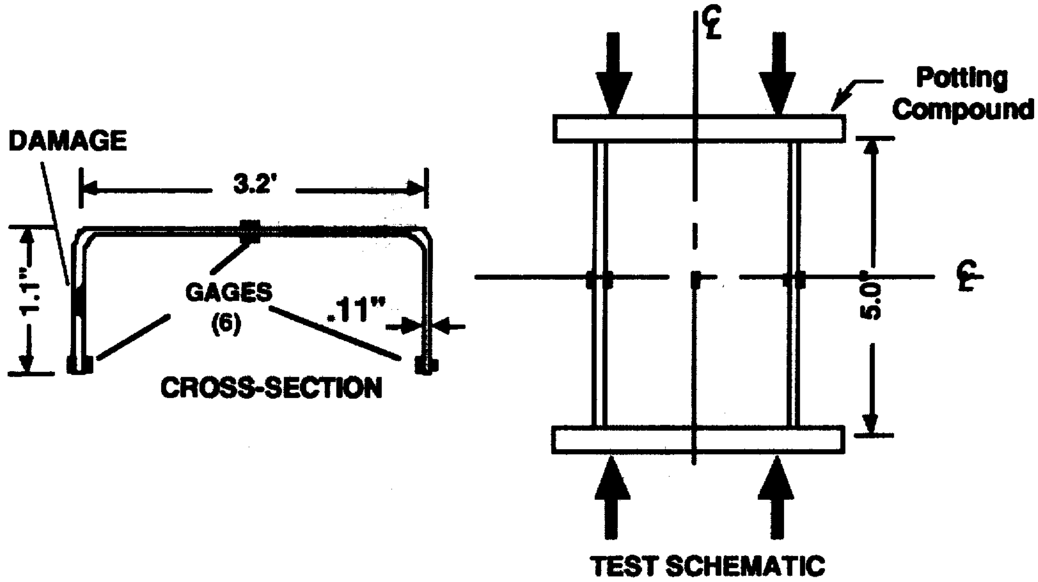

Figure 6 Crippling Test Specimen Configuration

RESULTS

Crippling Tests

During testing, all specimens buckled prior to final failure, with the web and flanges showing visible out-of-plane displacements. All specimens deformed into the shape of a one wave buckling mode, with the flanges usually opening up and the web bowing in; however, two of the undamaged LDF™ AS4/PEKK specimens experienced a change in buckling mode and switched to a two wave mode prior to failure after initially buckling in a one wave mode. In all undamaged cases, the failure sequence appears to be similar: the web starts buckling first, followed closely by the flanges. Buckling causes a rapid increase in bending strains which in turn causes an in-plane compressive failure of the flanges.

Based on NDI, impact damaged specimens showed some internal delaminations but no detectable fiber fracture. The failure mechanism for all damaged specimens appeared to be as follows: under compression loading the delaminated area under the impact site buckled locally, as indicated by the rapid increase in bending strain in the gage located next to the impact site, and delamination propagated rapidly to the specimen edge, leading to flange crippling and final failure. The appearance of the failed specimens was similar to their respective undamaged specimens, with the fracture originating at the impact site and the damaged flange showing more delamination.

As summarized in Figure 7, the undamaged LDF™ AS4/PEKK specimens failed at 42.5 ksi , while the AS4/3501-6 specimens failed in the flanges at an average stress of 41.8 ksi. The T800/F3900 specimens failed at an average stress of 58.5 ksi. After impact, failure occurred at an average stress of 28.6 ksi for the LDF™ AS4/PEKK specimens and 28.6 KSI for the AS4/3501-6 specimens. These both correspond to reductions of approximately 32% compared to the undamaged specimens. The damaged T800/F3900 specimens failed at an average stress of 48.8 ksi, a reduction of 17% compared to the undamaged specimens. These crippling test results are compared with compression ultimate coupon test results in Figure 8. All undamaged crippling test failures occurred at average stresses significantly below laminate ultimate strength, confirming the instability type failure.

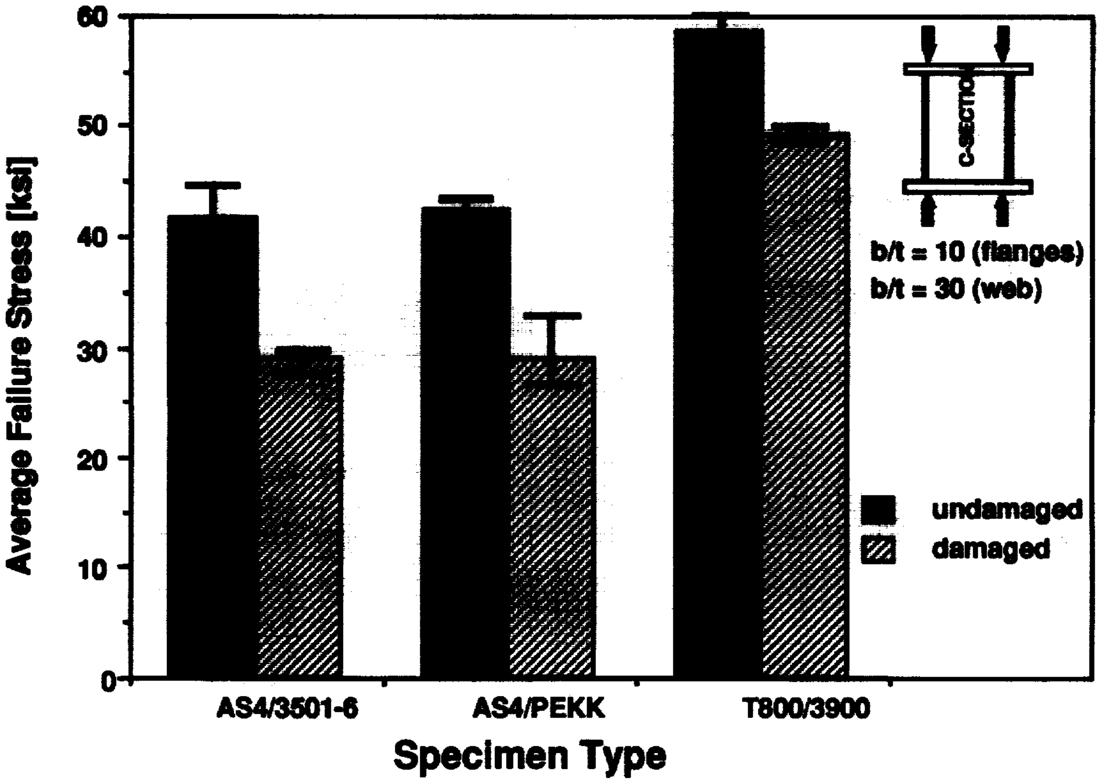

Figure 7 Average Crippling Stresses

Flange Bending Tests

Load versus displacement was recorded during testing. Indication of interlaminar failure could easily be identified by a sudden drop in load accompanied by clicking sounds. Some specimens exhibited a sudden and complete interlaminar failure of the flange, indicated by a load drop of 80% or more, while other specimens had an initial load drop of about 20%. After inspection, loading was resumed to final failure. No indication of any type of inplane damage could be seen in any specimen, thus indicating that the failure was purely interlaminar. The interlaminar tension stresses were determined for each specimen (Figure 8) and the results from these calculations for each specimen are shown graphically in Figure 9. The LDF™ AS4/PEKK material showed the highest average interlaminar tensile strength at 8200 psi, followed by the T800/F3900 at 5820 psi and the AS4/3501-6 at 4720 psi.

	TEST TYPE		
	Compression Ultimate	Channel Crippling	Flange Bending
Material System	STRESS (KSI) [CV%]	STRESS (KSI) [CV%]	STRESS(KSI) [CV%]
AS4/PEKK LDF™ Tape $[(\pm45)_2/0/90/\pm45/0/90]_s$ 20 plies (.108")	106 [8.4%]	42.5 [1.1%]	8.2 [6.4%]
AS4/3501-6 Fabric $[45_2/0_2/45_2/0]_s$ 14 plies (.105")	97.5 [4.4%]	41.8 [6.5%]	4.7 [8.4%]
T800/F3900 Fabric $[45_2/0/45/0]s$ 10 plies (.110")	83.5 [0.3%]	58.5 [3.7%]	5.7 [8.4%]

Figure 8 Average Strength Results

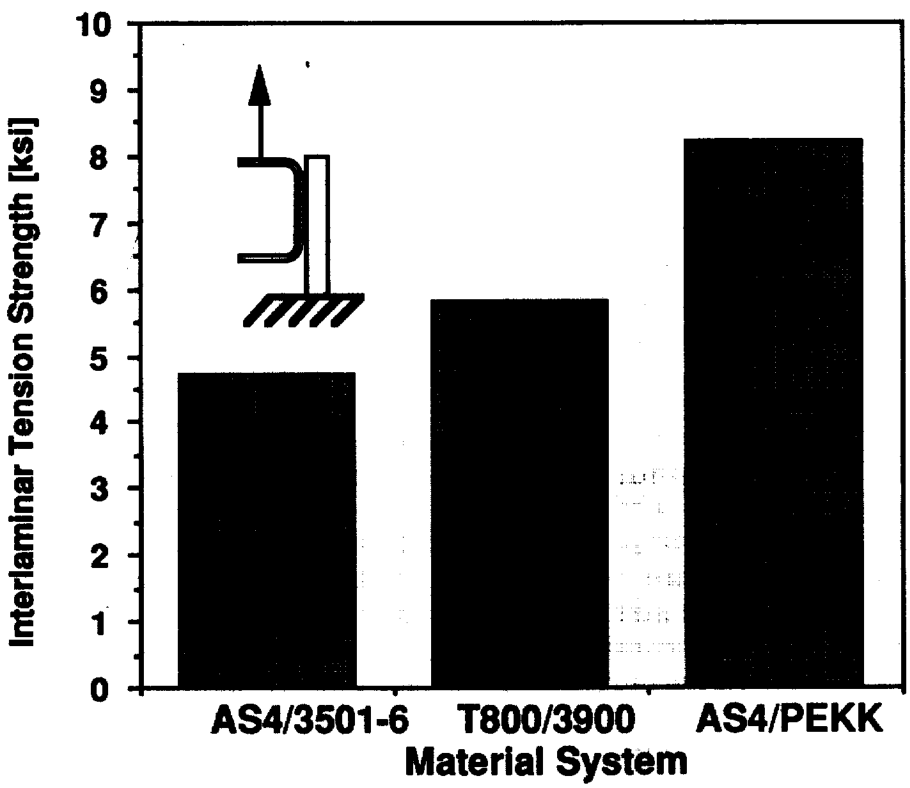

Figure 9 Summary of Average Interlaminar Tensile Strength

PHASE 3 FRAME TESTS

Frame Design

In Phase 3, a thin-gage fuselage frame section was manufactured through a stretch-forming operation. It is composed of two straight portions six inches long joined by a 45° circular bend with a 7.0 in radius; the width of the web is 1.6 in and the width of the flanges is 0.75 in. In order to evaluate the effect of layup, two layups were chosen which provide the same in-plane stiffness but different bending stiffness: $[\pm45/0/90/0_2]_s$ and $[0_2/\pm45/90/0]_s$. Three specimens of each kind were tested. Because of the high degree of draw in forming the curved part, additional 0° plies were added in the outer portion of the stock part. They were slightly longer than the entire curved portion of the part, insuring even stretching of the additional plies.

Frame Manufacturing

Stock Parts

Straight C channels were fabricated in matched steel tools (a fixed female and expandable 3-piece male tool). The LDF™ AS4/PEKK tape was layed-up on the male tool and then inserted in the fixed female tool. When pressure was applied to the tooling, the male tool expanded and forced the prepreg material to conform to the female tool. A 36 inch-square, 200 ton PHI hydraulic press supplied both the load and the heat required for consolidation.

Once the tooling and prepreg were loaded into the press, 5 tons were applied to insure adequate heat transfer. The pressure was increased to 45 tons (400 kN) once the process temperature of 700°F (370°C) was reached. This translates to about 750 psi (5.2 Mpa) on the part. When 700°F was reached, the platen heaters were turned off and the cooling cycle started. Pressure was maintained during cooling.

The channels were inspected by ultrasound and thickness measurements. Some variation in web and flanges thickness was observed. This was due to the design of the matched metal tools used to make the straight stock shape parts. The variation in stock shape thicknesses translated to variations in final part thicknesses.

Stretch Forming

The DuPont Research Stretch Former was designed and built to shape straight composite channels and beams into highly contoured parts. Matched metal tooling was developed to form the curved C channel. The straight C channel was inserted into the stretch forming machine and clamped in place. Electric heaters heated the part and the tooling to the process temperature of 700°F. Then the part was stretched and formed to the contour of the tool. After the stretching was complete, pressure was applied normal to the web and flanges to fully reconsolidate the part. With pressure still on the part, it was cooled to room temperature. The part was then removed from the machine and trimmed to final size using a bandsaw and wet grinder. Finally, it was ultrasonically inspected and the part checked for dimensions.

The high degree of draw (26%) required experimenting with ply buildups during the process development phase. A more detailed description of the stretch forming process can be found in US Patent No. 4,927,581 issued to the DuPont Company and titled "Method for Shaping Fiber Reinforced Resin Matrix Materials." Additional patents related to this process are pending. Both the straight and curved parts are shown in Figure 10.

Figure 10 Stretch Forming of LDF™ Frame

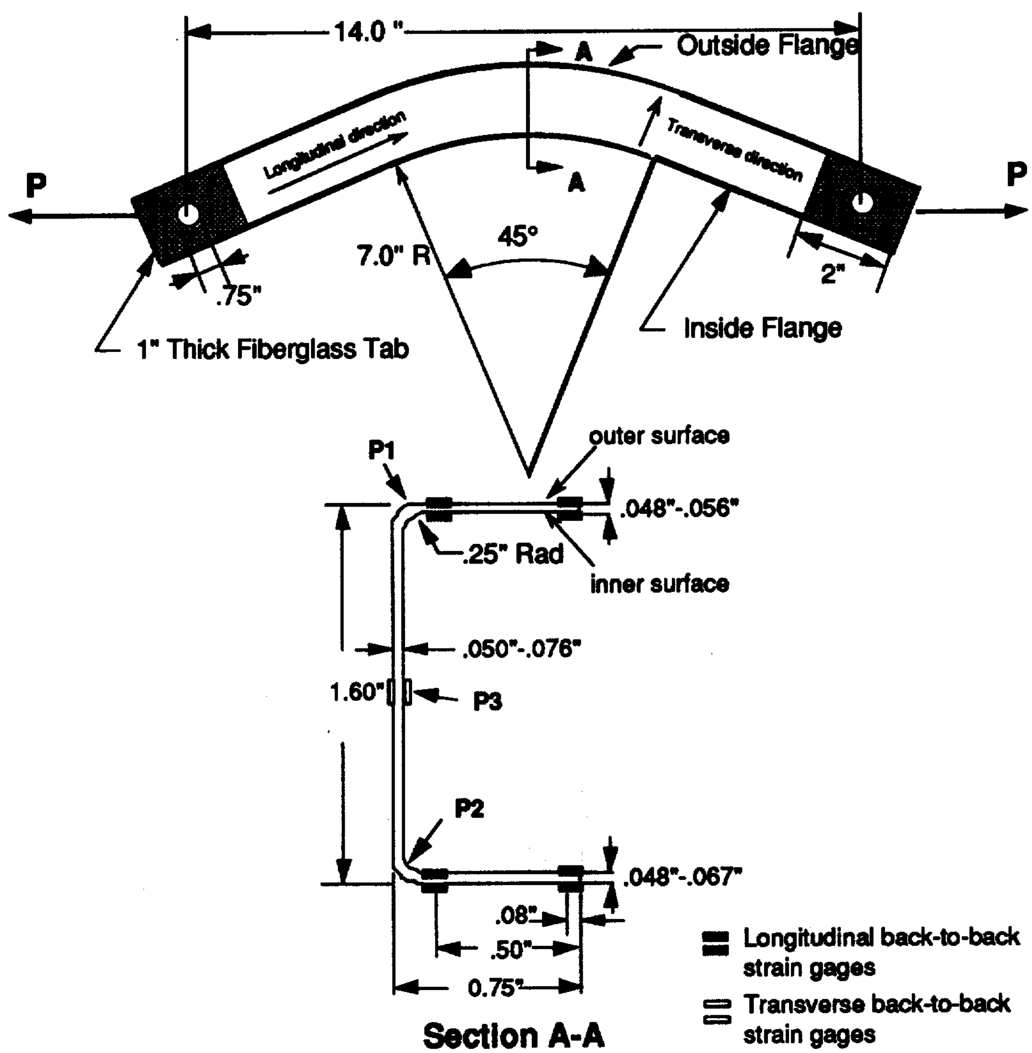

Figure 11 Curved Frame Specimen Configuration

Frame Test Method

Fiberglass/epoxy loading blocks, 1.0 inch thick by 2.5 inch long, were bonded to the inside surface at each end of the LDF™ stretched frame sections using EA9309.3 NA paste adhesive. Two holes (0.754 +/- .002) were drilled through the specimen, one in each of the two loading blocks, to provide a 14 inch separation between load application points. Final test specimen geometry is shown in Figure 11.

Several frames were tested as illustrated in Figure 12, to determine the strength of this LDF™ AS4/PEKK part after stretch-forming. The objective was to test the frame section under combined bending and axial loads while keeping the test setup fairly simple. Also, after reviewing the Phase 1 test data, a primary concern was the compressive strength of the LDF™ AS4/PEKK material after stretching. Therefore, the specimen was loaded in tension which avoided instability problems and allowed the stretched outer flange to be loaded in compression.

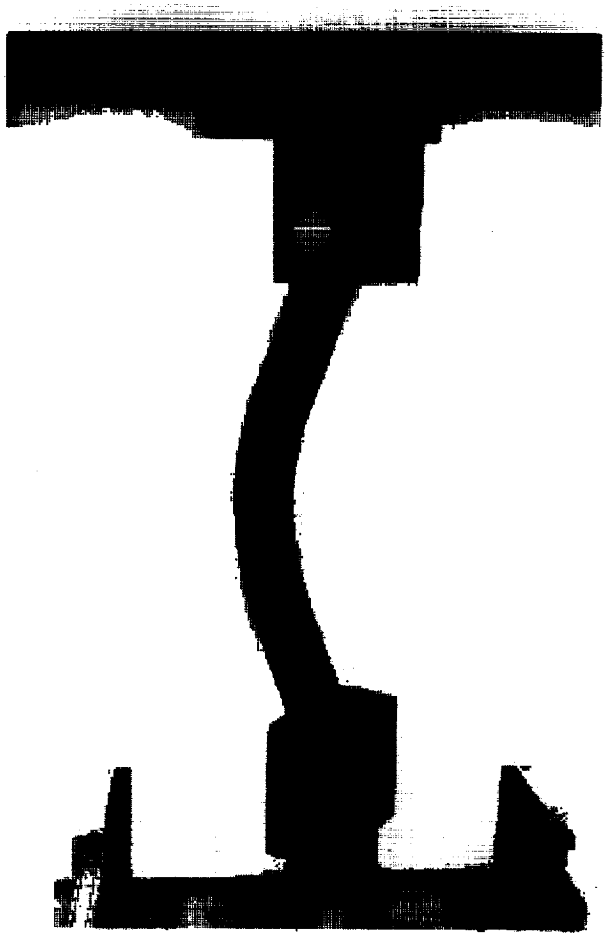

Figure 12 Frame Test Setup

Prior to testing, all specimens were instrumented with a number of strain gages. Testing was conducted in a 1127 Instron test machine with a 50,000 lb load cell. The specimens were loaded using a clevis at either end with a 0.750 inch diameter bolt. Load was applied at a constant rate until failure.

Experimental Results

During testing, large deformations of the flanges were observed in the curved section, with both flanges deforming outwards and opening up. Only a few clicking noises were heard during testing, some of which occurred at fairly low load levels and can probably be attributed to local failures in the adhesive bond of the tabs. No other significant noises were heard prior to final failure which was catastrophic in all cases. In four of the specimens, failure initiated on the tension side, in the curved section at the corner between the web and the inner flange and then propagated instantly around the cross-section with the specimen separating usually into two parts. In the remaining two specimens, failure initiated on the compression side at the corner between the web and the outer flange. A photograph of each kind of failed specimen is shown in Figure 13 and failure loads are given in Figure 14.

The following observations were made concerning the stress-strain behavior recorded during frame tests:

- The longitudinal strains at the tip of each flange are of opposite signs compared to the strains measured at the root of the same flange. This was due to the deformations of the flanges in the curved section.
- The longitudinal gages also show a slight stiffening behavior due to the fact the flanges are straightening in the curved section.
- The transverse gages on the web show a very nonlinear stiffening behavior: the reason is that the web is loaded transversely in tension, thus increasing the transverse bending stiffness of the web.

Frame Analysis

In order to better interpret the experimental results, a Finite Element (FE) model of the test specimen was generated using PDA's PATRAN modeler. PDA's FEA solver, P/FEA, was used for the analysis. A view of the analysis mesh is shown in Figure 15. The FE model consisted of 256 composite flat shell elements and was utilized to determine the ply longitudinal strain distribution at failure. Since strain gages could not be placed at the location of maximum strains, the model results were used to estimate the maximum tensile and compressive strains at failure for each specimen.

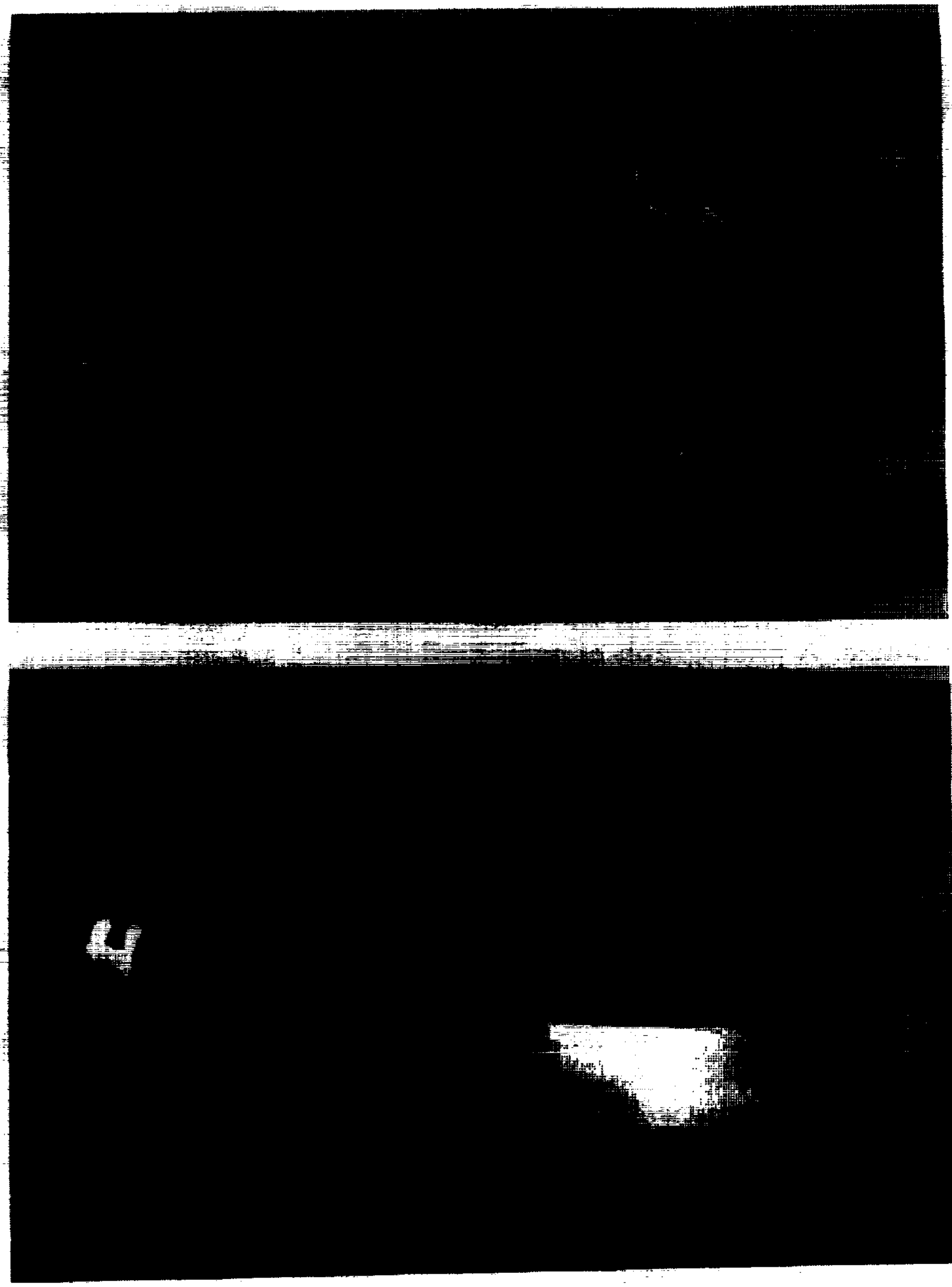

Figure 13 Frame Tensile (top) and Compressive (bottom) Failure Modes

The results of these strain calculations are shown in Figure 16. The ratios between model and experimental strains are also indicated. In Figure 17, the predicted strains around the frame cross-section are compared to strain-gage data. In general, the agreement is quite good for the membrane strain component, while there is more variation in the bending component since that measurement is more sensitive to local thickness variations. The predicted strain levels at failure in the specimens which experienced tension failures correspond well with the expected tensile strength of this material system (Phase 1 tests). Some reduction in compression strength compared to the unstretched Phase 1 test results was indicated in the specimens which failed in compression, due possibly to variations in

Specimen ID#	Layup	Outer Flange [in]	Web [in]	Inner Flange [in]	Failure Load [lb]	Failure Mode
B-130	$[\pm45/0/90/0_2]_s$	.052	.050	.048	1875	Tension
B-135	$[\pm45/0/90/0_2]_s$	.049	.076	.061	2450	Compression
B-149	$[\pm45/0/90/0_2]_s$	.051	.051	.062	1556	Tension
B-136	$[0_2/\pm45/90/0]_s$	.049	.062	.055	1870	Tension
B-143	$[0_2/\pm45/90/0]_s$	.056	.070	.065	2650	Tension
B-152	$[0_2/\pm45/90/0]_s$	.048	.071	.067	1915	Compression

Figure 14 Summary of Thicknesses and Failure Loads of Frames

the degree of reconsolidation of the material. Although some improvement in part to part consistency is needed, it is believed that this could be achieved with improved tooling. As illustrated in Figure 18, average test results show that the LDF™ AS4/PEKK structural properties after stretch-forming are not significantly different from the average failure strain levels obtained in tests of IM6/3501-6.

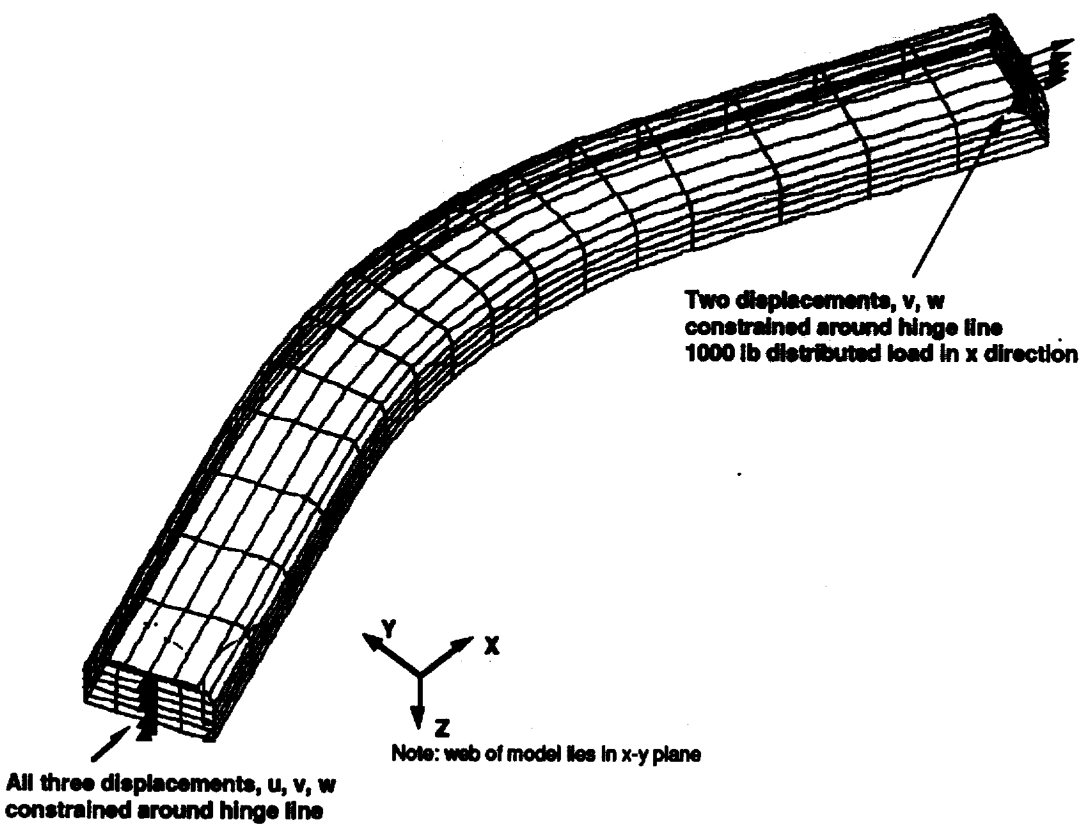

Figure 15 View of Curved Frame Finite Element Model

Specimen	Failure load [lb]	Model/Exper (membrane)	Model/Exper (bending)	Predicted Min. Strain at Failure	Predicted Max. Strain at Failure	Failure Mode (experiments)
B-135	2450	1.053	.69	**-8904**	12933	Compression
B-130	1875	1.06	.85	-8630	**13550**	Tension
B-149	1555	.80	.90	-8342	**13764**	Tension
B-136	1870	.99	1.12	-8672	**12777**	Tension
B-143	2650	1.13	.47	-9861	**14840**	Tension
B-152	1915	.94	.45	**-8765**	12650	Compression
Mean	2053	.99	.75	-8862	13419	
Std. Dev.	411 (20%)	.04 (4%)	.10 (13%)	523 (6%)	824 (6%)	

Figure 16   Curved Frame Predicted Maximum and Minimum Strains

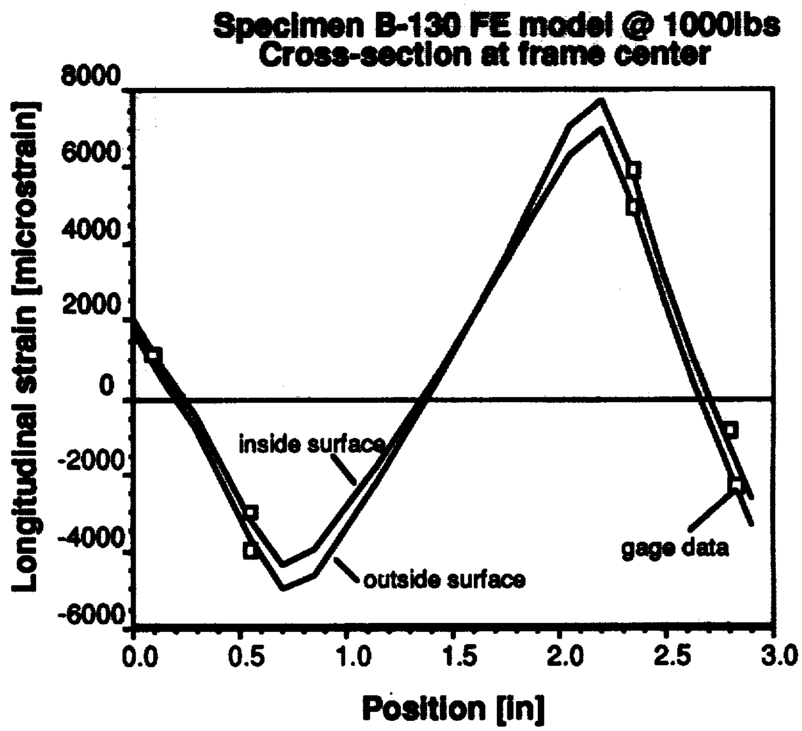

Figure 17   FEM Strains Compared to Experimental Data

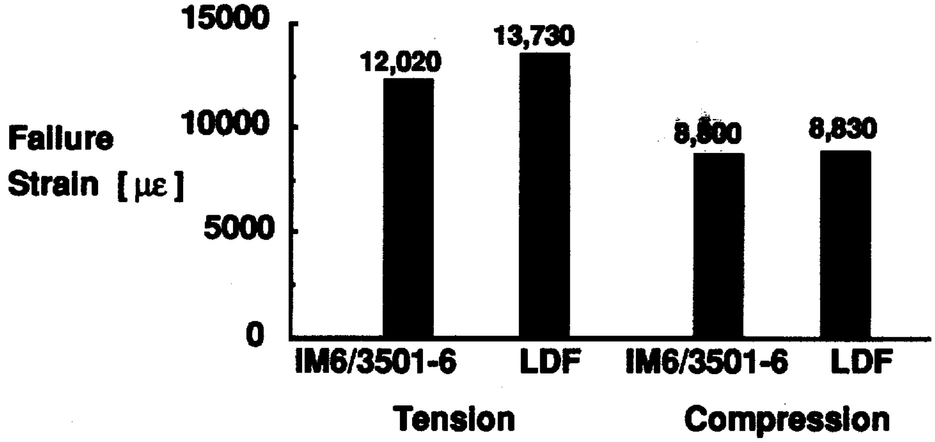

Figure 18 Comparison of LDF™ AS4/PEKK and IM6/3501-6 Average Strain Levels

FRAME COST STUDY

A cost study was conducted on the frame manufactured and tested in Phase 3. Included in the estimates of average unit cost was both recurring (labor, material) and non-recurring (tooling) costs for the manufacture of 1300 frames. Capital expenditures were omitted. The baseline, hand lay-up of a thermoset frame, requires 3 pieces to be assembled. Figure 19 is a schematic of this frame section. BH Industrial Engineering applied an 83% learning curve to these parts. Two potential material costs were used; \$50 representing current AS4/3501-6 cost and \$70 representing estimates of toughened thermoset cost. The LDF™ part, estimated by DuPont, is one-piece and uses a 90% learning curve reflecting the more automated process. Two material cost extremes were again utilized; \$110 reflecting current thermoplastic prepreg cost and \$60 reflecting large production estimates. Results are shown in Figure 20. Based on tooling costs, the unit LDF™ cost is higher for very small lot sizes. For 1300 parts the use of LDF™ for this frame results in a 43-59% savings, depending on individual material costs used.

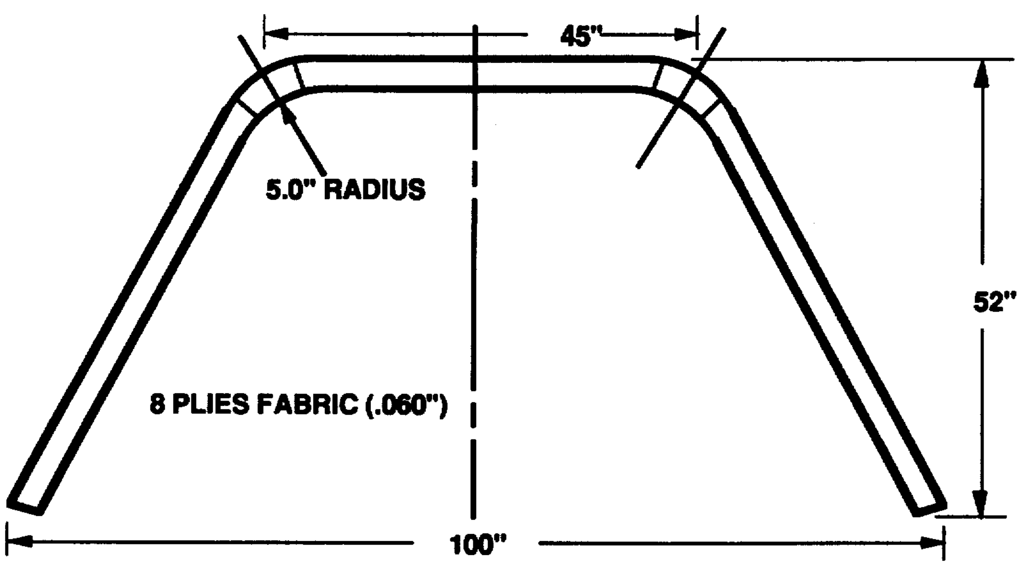

Figure 19 Frame Section in Estimate

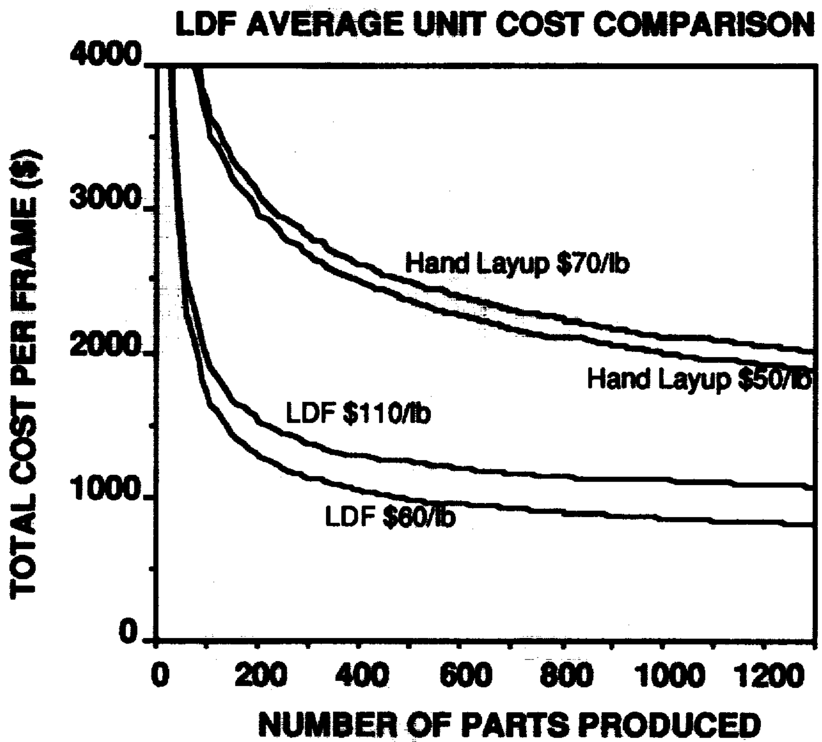

Figure 20 Cost Estimates of Frame Manufacture

CONCLUSIONS

The stretch forming of an LDF™ AS4/PEKK frame was successfully demonstrated in this investigation. It is believed that this process is feasible for thin curved rotorcraft frames and offers a significant cost advantage over the hand lay-up of thermoset frames while not compromising overall part strength. Specific conclusions are as follows:

- Material properties test results agree with values previously reported. All tensile properties for LDF™ AS4/PEKK compared favorably with those of continuous fiber AS4/PEKK composites, while compressive strength properties showed a small drop for unstretched LDF™. Low compression strength properties were obtained due to the poor quality of the stretched specimens, these results also indicating that adequate reconsolidation of the part after stretching is an important factor.
- Channel crippling tests showed similar strength results for LDF™ tape layup and continuous fiber AS4/3501-6 fabric layup. Crippling strength of high-strain graphite/toughened thermoset fabric (T800/F3900) layup was higher due to the higher modulus and strength of the fiber. Crippling tests of impact-damaged specimens showed no significant difference between the AS4/thermoset fabric and the LDF™/PEKK tape, while the toughened thermoset material showed an improvement in damage tolerance.
- Flange bending tests showed that PEKK has the highest interlaminar tensile strength, followed by the toughened thermoset F3900 and the epoxy matrix 3501-6.
- The feasibility of stretch-forming curved frame section was demonstrated. Although some improvements in part consistency are still needed (better tooling), structural testing showed only a small reduction in strength due to the manufacturing process.

- Regardless of the material cost used in the calculations, the stretch forming of LDF™ composites results in a lower cost manufacturing process compared to hand lay-up for large lot sizes.

ACKNOWLEDGMENTS

The authors would like to gratefully acknowledge the contributions of other Helicopters Division and DuPont personnel who contributed to this effort. Christian Gunther's and and Jim Pratte's guidance was instrumental in the experimental investigation and final report preparation.

REFERENCES

1. Khan, S., Pratte, J.F., Chang, I.Y., and Krueger, W.H., "Composites for Aerospace Application from Kevlar Aramid Reinforced PEKK Thermoplastic", Presented at the 35th International SAMPE Symposium, Anaheim, California, April 2-5, 1990.

THIS PAGE INTENTIONALLY BLANK